Optica Applicata, Vol. LII, No. 2, 2022
DOI: 10.37190/oa220208

Real time motion compensation technology based on least square support vector machine prediction

ZHEHAN SONG, HUAJUN FENG, ZHIHAI XU, QI LI*

College of Optical Science and Engineering, Zhejiang University, Hangzhou 310012, China

*Corresponding author: liqi@zju.edu.cn

When cameras are used in aerial photography, satellite imaging or other scenes, the motion of the observational target causes image blur. The corresponding motion compensation systems often present some response delay. Thus, we introduce effective and fast motion prediction for the target to achieve steady real-time motion compensation. We first analyze the target motion states to propose a fast and robust prediction method based on the least square support vector machine algorithm. Then, we evaluate the performance between ours and other state-of-the-art methods through experiments. Experimental results confirm that the proposed method provides a fast and robust prediction for target motion. At last, we embed our method with dual-resolution camera system to perform high-quality motion compensation effect in real time.

Keywords: motion compensation, motion prediction, dual-resolution camera system, least square support vector machine.

1. Introduction

When a camera images to a moving target, the movement of the observational target causes motion blur, rendering compensation essential under such conditions.

Many compensation methods have been proposed to address such motion blur. They can be categorized as those that compensate motion blur [1–7] using the sensor and system which are made to follow the moving object, and those that restore the deteriorated image in post-processing [5,6,8–12]. As a method of the former category, time delayed integration (TDI) extends the exposure time virtually [1]. So with the target speed increasing, every stage of TDI exposure time will decrease which limits practical application. HAYAKAWA *et al*. [7] propose a real-time compensation system with optical gaze control using a galvanometer mirror. Another method of the former category is based on optical image stabilization [2,3] with lower accuracy. As for the latter category, blind deconvolution [6,8,9] estimates point spread function from captured

images offline. Motion vectors can also be easily got [5, 10–12] to achieve faster compensation. Different from getting motion vectors by using a hardware (flutter shutter) [5], ZHONG *et al*. [11] applied motion estimation technology which also can be named as electronic image stabilization. KUMAR *et al*. [12] explored a faster motion estimation method for image stabilization. Obviously the latter category cannot capture real-time restored images and the former needs precision instruments and is limited by the object speed. Generally, the former is better than the latter because it can compensate the object motion at once, but the latter gets more accurate motion vectors. Thus, we combine motion prediction algorithms integrated with electronic image stabilization methods to propose a new motion compensation technology which accesses advantages of both the former and the latter.

Traditional motion prediction algorithms [13–18] include the autoregressive integrated moving average (ARIMA) model, Kalman filter, least squares support vector machine (LSSVM) and Markov model etc. PREVOST *et al*. [13] apply extended Kalman filter to moving object trajectory prediction by introducing nonlinear units. FU *et al*. [14] combine genetic algorithm with LSSVM to converge more quickly. ZHAO *et al*. [15] explore the second order Markov model for motion prediction which associates the current state with historical data to improve the model robustness under sudden changes. GUO *et al*. [16] update a data-driven ARIMA model to predict vehicle velocity by collecting real-time historical data. Least squares support vector machine (LSSVM) maps data onto a high-dimensional space before modeling, thus being able to handle complex systems.

Recently, motion prediction algorithms based on neural networks [19, 20] have been devised to provide accurate results. For instance, the backpropagation neural network (BPNN) uses neuron superposition during calculations and nonlinear activation to minimize the error between the predicted and true values. CHENG *et al*. [20] simplify network structure for accelerating ship motion prediction. Similarly, long short-term memory (LSTM) networks [21, 22] use approach such as forgotten door mechanism for combining past cells states to determine the current cell state. LSTM method [22] combing with state refinement enables researchers to predict complex pedestrian motion trajectory. Clearly, LSTM networks are more robust than BPNNs. Overall, the robustness and accuracy achieved by neural networks are higher than those achieved by conventional algorithms, but the neural network complexity is also higher.

So we introduce a motion prediction model leveraging both complexity and accuracy. After analyzing the states of a moving target in different situations, we propose an improved LSSVM for motion prediction. We then compare the proposed method with conventional algorithms and neural networks, namely, ARIMA model [16], Kalman filter [17], online LSSVM [18], BPNN [20] and LSTM network [21]. The comparison results show that the proposed LSSVM outperforms the other methods regarding prediction speed and accuracy. We finally develop the corresponding dual-resolution camera system and realize our algorithm based on this system which achieves effective motion compensation in real time.

2. Analysis

In this section, we explain the reason of using motion prediction combined with motion vector estimation which can achieve real-time motion compensation.

Since motion compensation based on electronic image stabilization presents delays between the high-speed image acquisition and the motion vector calculation, it consequently hinders real-time motion compensation to obtain clear images. Figure 1 illustrates the timing of camera detection, motion estimation, and motion compensation. As motion estimation takes time, only when frame n-1 is acquired, the motion estimation of frame n-2 is completed. Then, when frame n is acquired, the compensation of frame n-2 is completed.

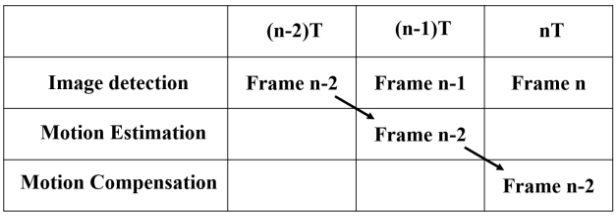

Fig. 1. Timing of image detection, motion estimation, and motion compensation.

Motion compensation is delayed by two time steps after image acquisition. Thus, when frame n is acquired, we can use motion vectors before frame n-2 to predict the motion vector of frame n. Finally, the predicted motion vector of frame n is transferred to perform motion compensation without delay. Considering that estimation, prediction, and compensation should be completed in one exposure period, a fast and robust motion prediction method should be achieved.

In the process of camera detection, the movement state of the target may change at any time. Although the complete target motion form is unpredictable, the target motion in a short time can be predicted by models which also explains why dual resolution camera system has a high frame-rate plane, in Section 4. Overall, the target in a short time has two main states of steady moving and sudden shifting.

Considering the possible movement state of the target in a short period of time, we propose a method for fast and robust target motion prediction.

3. Methods

3.1. Online LSSVM

Consider a training set $\{(x_1, y_1), (x_2, y_2), ..., (x_n, y_n)\}$ with n training samples. The conventional LSSVM uses nonlinear function φ to map the input samples onto a high-dimensional feature space. Then, the nonlinear estimation in the original low-dimensional sample space is converted into linear estimation in the high-dimensional feature space:

$$f(x) = w^{\mathrm{T}}\varphi(x) + b \tag{1}$$

where w and b represent the mapping coefficients and bias, respectively, $f(x)$ is the high -dimensional feature space function. LSSVM introduces laxity variable $\xi = (\xi_1, ..., \xi_n)$ to convert this regression problem into a constrained minimization problem:

$$\min J(w, \xi) = \frac{1}{2}\|w\|^2 + \frac{\gamma}{2}\sum_{i=1}^{n}\xi_i \tag{2a}$$

$$s.t. y_i = w^{\mathrm{T}}\varphi(x) + b + \xi_i, \quad (i = 1, 2, ..., n) \tag{2b}$$

where J is the minimization cost function and γ is a penalty coefficient.

To solve the minimization problem above, Lagrange multipliers $\lambda = (\lambda_1, ..., \lambda_2)$ are used to express the problem as an unconstrained optimization problem. The Lagrange equation is given by

$$L(w, b, \xi, \lambda) = J(w, \xi) - \sum_{i=1}^{n}\lambda_i\left[w^{\mathrm{T}}\varphi(x) + b + \xi_i - y_i\right] \tag{3}$$

whose equations can be obtained by applying the following Karush–Kuhn–Tucker conditions:

$$\frac{\partial L}{\partial w} = w - \sum_{i=1}^{n}\lambda_i\varphi(x_i) = 0 \tag{4a}$$

$$\frac{\partial L}{\partial b} = -\sum_{i=1}^{n}\lambda_i = 0 \tag{4b}$$

$$\frac{\partial L}{\partial \xi_i} = \lambda_i - \gamma\xi_i \tag{4c}$$

$$\frac{\partial L}{\partial \lambda_i} = w^{\mathrm{T}}\varphi(x_i) + b + \xi_i - y_i = 0 \tag{4d}$$

The expressions in (4) can be represented in matrix form as follows:

$$\begin{bmatrix} 1 & 0 & 0 & -\varphi \\ 0 & 0 & 0 & -I \\ 0 & 0 & \gamma I & -I \\ \varphi & I & I & 0 \end{bmatrix}\begin{bmatrix} w \\ b \\ \xi \\ \lambda \end{bmatrix} = \begin{bmatrix} 0 \\ 0 \\ 0 \\ y \end{bmatrix} \tag{5}$$

where 1 denotes an n-element vector of ones, I denotes the identity matrix with n-dimensions, and $\varphi = (\varphi(x_1), ..., \varphi(x_n))^{\mathrm{T}}$.

To simplify (5), the kernel trick can be used to map the nonlinear primitive function onto a new feature function. For any two input samples (x_i, x_j), the kernel trick is expressed as $k(x_i, x_j) = \varphi(x_i) \times \varphi(x_j)$.

Considering (4), (5), and the kernel trick, the corresponding matrix expression is given by

$$\begin{bmatrix} 0 & I^{\mathrm{T}} \\ I & k + I/\gamma \end{bmatrix} \begin{bmatrix} b \\ \lambda \end{bmatrix} = \begin{bmatrix} 0 \\ y \end{bmatrix} \tag{6}$$

where λ and b are the LSSVM regression coefficients. Online LSSVM replaces all data with data in sliding window to speed up model solving which is finally given by (7), L is the sliding window length.

$$g(x) = \sum_{i=1}^{L} \lambda_i k(x, x_i) + b \tag{7}$$

3.2. Proposed LSSVM

Our improved LSSVM is based on the model in (7). Thus, real-time training and prediction can be achieved regardless of the size of the training set.

Regression coefficient λ is a vector with the same length of the training set and allocates different weights to the samples, thus being a weight vector. Using (4), we obtain

$$\lambda = \gamma \xi \tag{8}$$

The elements in the weight vector are proportional to the laxity factor, which reflects the deviation of the data from the fitted curve. Faster data changes imply higher weights, whereas smoother changes imply that the maximum weight is closer to the endpoint. We can explain the weight matrix considering gradients. Given two adjacent data points $\{(x_1, y_1), (x_2, y_2)\}$, their gradient t is given by (9) and represents the rate of data variation.

$$t = (y_2 - y_1)/(x_2 - x_1) \tag{9}$$

When data vary according to an internal law, the left gradient is close to the right one. Meanwhile, one side of the endpoints has no derivative, and thus the endpoint data have the highest weight. As the laxity factor is negative, the absolute value of the endpoint weight is the highest.

When the data behavior changes suddenly, the left and right gradients are considerably different. The largest value of the weight vector is assigned to the most variable data point. However, the weighting of sudden changes is not sufficient because noise and small fluctuations also affect data. Thus, we measure the data variation to identify sudden changes by defining a gradient matrix.

Let S be a data sequence, the length of the sliding window be N, and consider m consecutive data points before time t to predict the data two time steps ahead. The following equations can be used to train pairs of data points (X, Y):

$$X = (S_{t-m+1}, ..., S_t)^{\mathrm{T}} \tag{10a}$$

$$Y = S_{t+2} \tag{10b}$$

The final input training data point, (X_r, Y_r), is given by:

$$X_\mathrm{r} = \begin{bmatrix} S_1 & ... & S_{N-m-1} \\ ... & ... & ... \\ S_m & ... & S_{N-2} \end{bmatrix} \tag{11a}$$

$$Y_\mathrm{r} = (S_{m+2}, S_{m+3}, ..., S_N)^{\mathrm{T}} \tag{11b}$$

Then, we use matrix X_r to construct gradient matrix G as follows:

$$G = \begin{bmatrix} S_2 - S_1 & ... & S_{N-m-1} - S_{N-m-2} \\ ... & ... & ... \\ S_{m+1} - S_m & ... & S_{N-2} - S_{N-3} \end{bmatrix} \tag{12}$$

Each column of G is obtained by subtracting two adjacent columns of matrix X_r. Thus, every element of G can be treated as the gradient of the corresponding point.

Matrix G should be sensitive to sudden changes and robust during normal prediction. Thus, we sum every column of G to obtain the following row vector:

$$G_\mathrm{r} = (G_1, G_2, ..., G_{N-m-2}) \tag{13}$$

Each element of vector G_r denotes the gradient sum of m consecutive data points. Then, we define T_r as follows:

$$T_\mathrm{r} = \min(G_\mathrm{r})/\max(G_\mathrm{r}) \tag{14}$$

T_r being below a threshold T indicates that the state has suddenly changed, and the data point with the maximum weight is considered as the changing point. Finally, we crop the training data to discard the changing point and then reconstruct the training matrix and perform the prediction.

4. Dual-resolution camera system

Since a single-resolution camera system has only one imaging plane, it is not only need to use this image plane for motion estimation and prediction, but also to compensate the

target movement in the same image plane in real time. When the target motion speed is fast, two problems will be introduced: 1) The result of motion estimation will produce a large error, which will affect the effect of real-time motion compensation. 2) Due to the limitation of imaging time, motion estimation cannot obtain the exact target motion state within one frame of imaging period.

Therefore, we design a dual resolution camera system with common light path structure which means two image planes share one optical system. The whole system applies motion estimation and motion prediction modules to an additional high frame-rate image plane, and the original image plane only performs motion compensation. The system schematic diagram is designed as shown in Fig. 2.

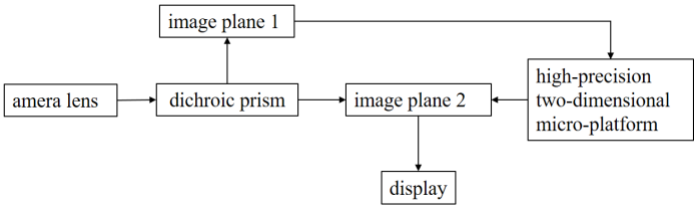

Fig. 2. Schematic diagram of dual-resolution camera system.

The whole system of images is presented as the form of fixed focus length 152 mm and *F*-number of the camera lens is 2.6. The incident light passing through the lens is split to two paths by a dichroic prism (split ratio is 3 to 7). One path is received by high frame-rate image plane 1 and the other is received by high-resolution image plane 2. The high frame-rate image plane 1 sends the calculated value to the high-precision two -dimensional micro-platform. The high-precision two-dimensional micro-platform moves the high-resolution image plane 2 to achieve the purpose of compensating the target motion. In this case, the system can repeatedly compensate for a fast moving target by high frame-rate image plane 1 and obtain clear motion compensation of the target by high-resolution image plane 2. The final three views of dual-resolution camera system are shown in Fig. 3.

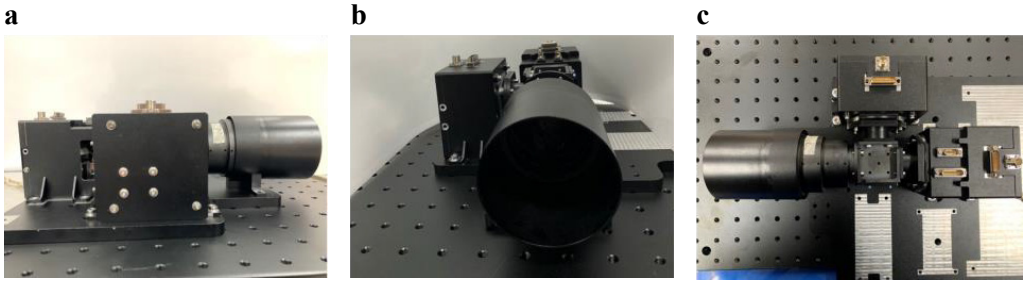

Fig. 3. Three views of dual-resolution camera system. (**a**) Left view, (**b**) front view, and (**c**) top view.

5. Experiments

5.1. Evaluated parameters

We used the following parameters and configurations for experiments. For evaluating motion prediction methods, we set N and m equal to 9 and 3, respectively, and used a Gaussian kernel function with a variance of 0.6. In addition, we set threshold T equal 0.6.

For evaluating motion compensation effect of dual resolution camera system, the frame-rate of high frame-rate and high resolution image plane are 100 and 12.5 fps, respectively. Therefore, when we obtain a compensated high-resolution image, it has actually been compensated eight times. Compared with the single compensation of a single resolution camera system, the compensation accuracy can be greatly improved.

5.2. Evaluation on the videos obtained by dual-resolution camera system

We built an experimental environment to evaluate the motion prediction methods. The whole devices include a dual-resolution camera system, a resolution board, a voltage generator, and a motion generator.

The voltage generator generated different modulation voltages to control the motion generator to pull the resolution plate to generate sinusoidal motions with different amplitudes and frequencies.

The ground-truth of target motion was obtained by gray-scale projection [21] and linear interpolation which was also the corresponding motion estimation method embedded in dual-resolution camera system.

We first conducted experiments during stable operation. We continuously captured multi-frame images to obtain the target motion. Figures 4**a**–4**f** show the motion pre-

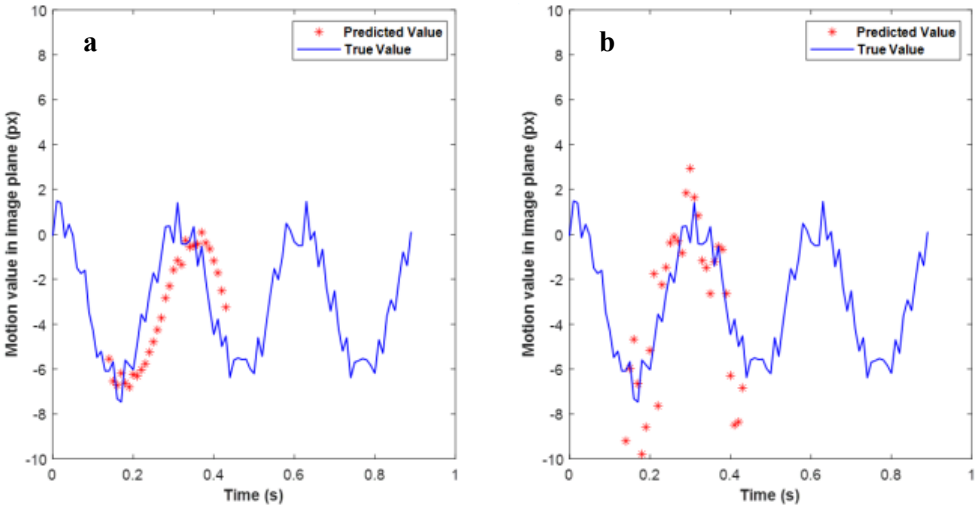

Fig. 4. Experimental results for stable operation. (**a**) Kalman filter, (**b**) ARIMA, (**c**) online LSSVM, (**d**) BPNN, (**e**) LSTM, and (**f**) our method.

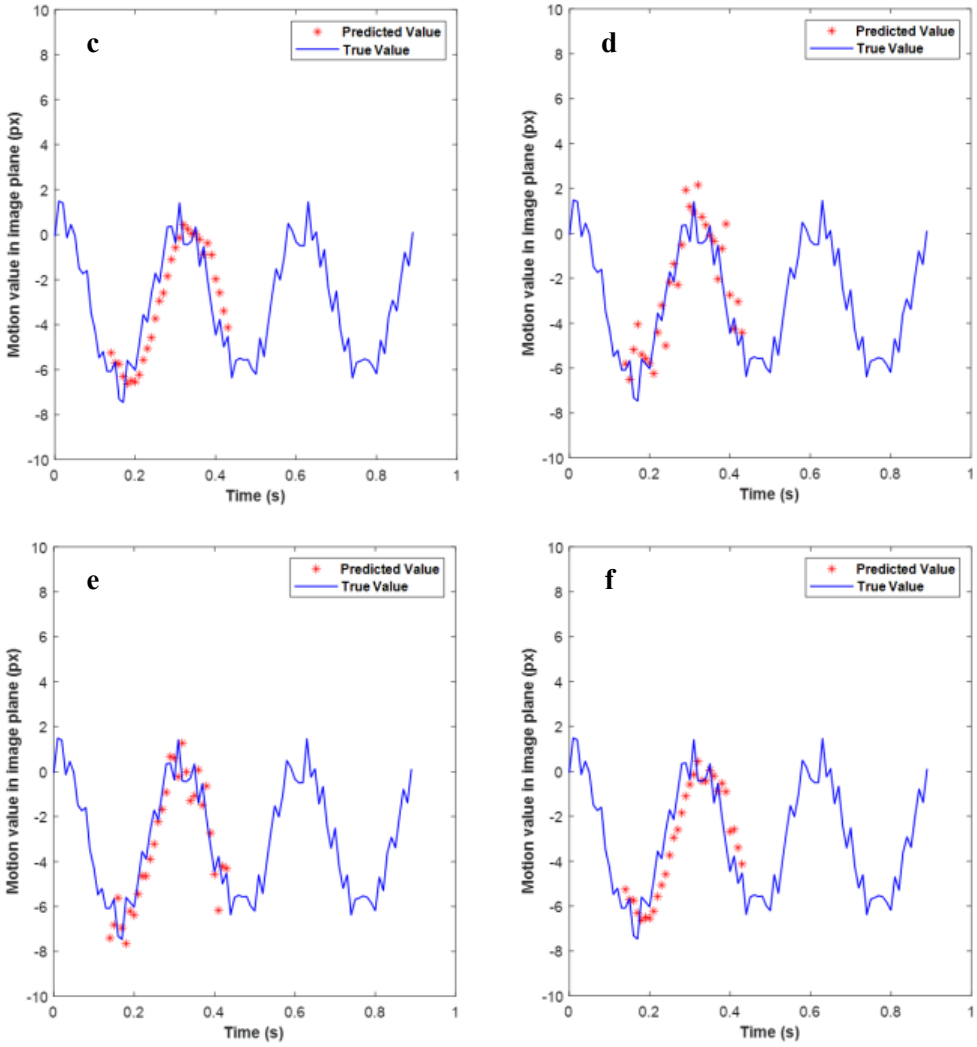

Fig. 4. Continued.

diction results of the Kalman filter, ARIMA model, Online LSSVM, BPNN, LSTM network, and the proposed LSSVM, respectively. The results of the ARIMA model fluctuate widely, indicating its low robustness. The Kalman filter shows a small delay. Our proposed method and LSTM network converge better than the other methods.

We then conducted experiments with the observational target under sudden shifting. During image acquisition, we modified the voltage to apply an external change to the target motion.

The prediction results of the evaluated methods are shown in Figs. 5**a**–5**f**. The Kalman filter, BPNN and Online LSSVM provide a suitable prediction before the disturbance.

The ARIMA model is still influenced by noise. However, when the disturbance is applied, the methods of Kalman filter, BPNN and Online LSSVM provide a poor prediction effect and can only converge to the data after a long period.

Only the LSTM network (Fig. 5**e**) and proposed LSSVM (Fig. 5**f**) are robust regardless of the large disturbance, and both methods converge quickly afterward.

Table 1 lists the mean squared errors of the evaluated methods. The proposed method achieves the highest performance, which is comparable to that of the LSTM network.

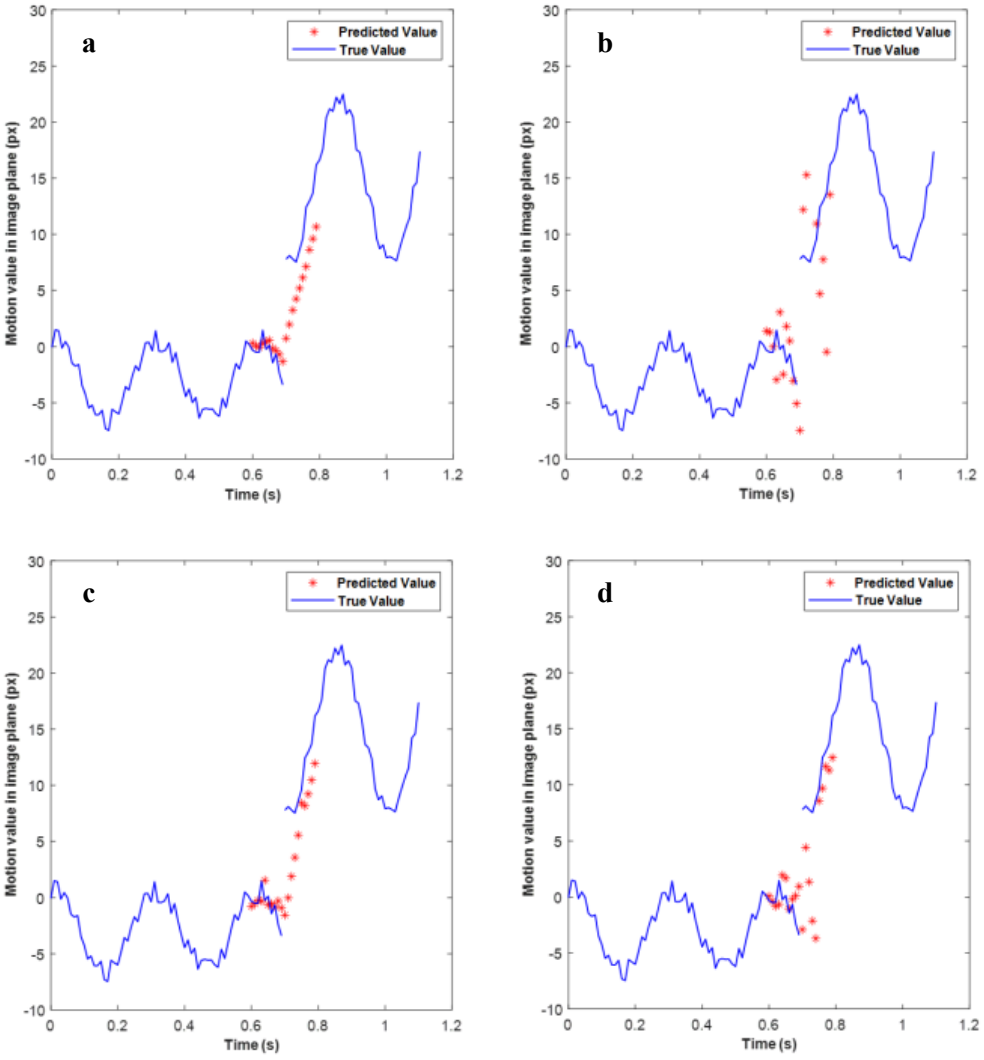

Fig. 5. Experimental results for sudden change. (**a**) Kalman filter, (**b**) ARIMA, (**c**) online LSSVM, (**d**) BPNN, (**e**) LSTM, and (**f**) our method.

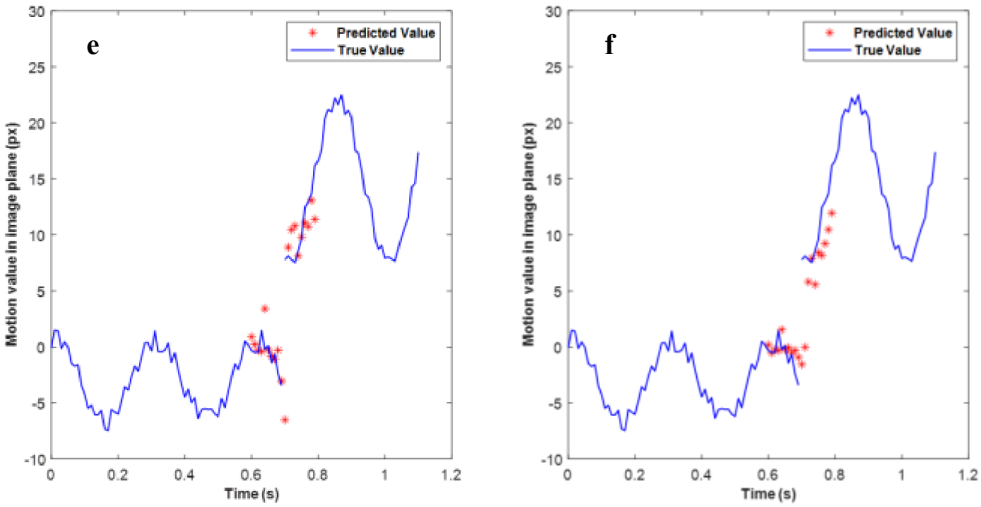

Fig. 5. Continued.

T a b l e 1. Mean squared error.

Mean square error	Stable operation	Sudden shifting
Kalman filter	4.09	16.72
ARIMA	5.05	83.95
Online LSSVM	1.77	16.35
BPNN	2.30	24.10
LSTM	1.67	13.87
Ours	1.63	13.42

The average running time of our method is 0.0013 s. Only Kalman filter (0.0018 s) and online LSSVM (0.0011 s) can compare with our method. The average running time of ARIMA, BPNN and LSTM are 1.21, 0.32 and 2.11 s, respectively. Our method can be well equipped with dual-resolution camera system.

5.3. Evaluation on dual-resolution camera system

We finally embedded the proposed algorithm in the dual-resolution camera system. During imaging, the object distance is 4.5 m and the resolution board horizontally moved in the field of view at different motion speeds (Corresponding to different image plane motion speeds).

Since the maximum image plane motion speed that can be compensated by the high-precision two-dimensional micro-platform is 0.522 mm/s, we evaluated final results by operating target at different image plane motion speeds which are 0.2, 0.35 0.5 mm/s, respectively. The stationary resolution board image can be distinguished to scale 11.

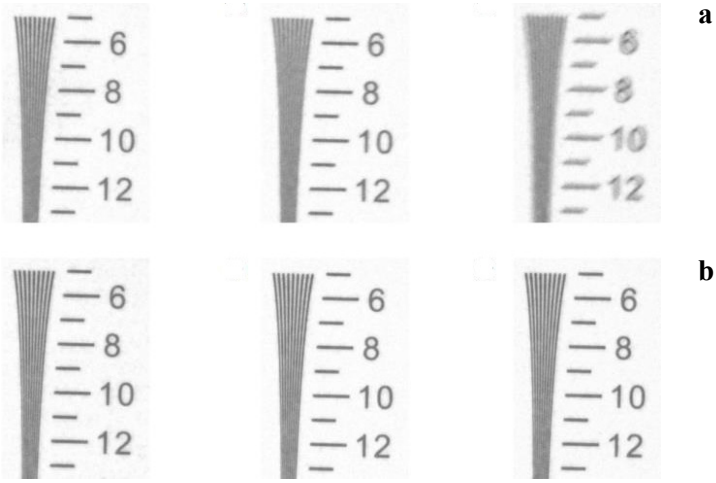

Fig. 6. Comparison results of motion blur and motion compensation under different image plane motion speeds. (**a**) Motion blur, and (**b**) motion compensation.

Figure 6 shows the comparison results of the motion-blurred image and the motion -compensated image when image plane motion speed is 0.2 mm/s and increases to 0.35 and 0.5 mm/s. As speed increases, corresponding motion blur images (Fig. 6**a**) quality becomes worse until it is difficult to distinguish any scale on the target. However, motion-compensated images (Fig. 6**b**) can be distinguished to scale 11, the same as the stationary target image quality.

As shown in Table 2, we also calculated the MTF value of motion-blurred and motion-compensated images at 0.5 normalized Nyquist frequency to further confirm compensation effect. The MTF value of stationary image equals 0.2.

T a b l e 2. MTF value.

Image plane motion speed	Motion-blurred	Motion-compensated
0.2 mm/s	0.14	0.2
0.35 mm/s	0.08	0.2
0.5 mm/s	0.03	0.2

The maximum image plane motion speed which our system can fully compensate is 0.522 mm/s. When imaging a target at 4.5 km, the maximum relative motion speed that the system can fully compensate is 55.62 km/h which is suitable for compensating the motion of space and remote sensing targets

At last, we evaluate the limit image plane motion speed that can be compensated, which is 0.65 mm/s. Converting to 4.5 km object distance, the maximum relative motion speed that the system can respond to and effectively compensate is 69.25 km/h.

6. Conclusions

The dual-resolution camera system can provide high resolution for the target we are interested in, which can be well applied to space observation and other applications. However, target motion will incur severe motion blur. Recent motion prediction methods can hardly be integrated with this system because of the limitation of precision and speed. We therefore propose a fast and robust motion prediction method for dual-resolution camera system to achieve excellent real-time motion compensation effect. Regarding prediction accuracy, the proposed method outperforms the Kalman filter, BPNN, online LSSVM, and ARIMA model while providing competitive results to the LSTM network. Regarding prediction speed, the proposed method is at least two orders of magnitude faster than the LSTM network. Experiments demonstrate the effectiveness and robustness of the proposed LSSVM. Since the compensation capability of this system is closely related to the high-precision two-dimensional micro-platform and computing power of the embedded algorithm, we will consider further improving the pulse frequency of the high-precision two-dimensional micro-platform and optimizing the embedded algorithm.

Acknowledgements
This work was supported by Zhejiang University Basic Research Projects (2018110C081), and we thank Meijuan Bian from the facility platform of optical engineering of Zhejiang University for instrument support.

References

[1] Bodenstorfer E., Furtler J., Brodersen J., Mayer K. J., Eckel C., Gravogl K., Nachtnebel H., *High-speed line-scan camera with digital time delay integration*, Proc. SPIE **6496**, Real-Time Image Processing 2007, 64960I (26 February 2007), DOI: 10.1117/12.704516.

[2] Golik B., Wueller D., *Measurement method for image stabilizing systems*, Proc. SPIE **6502**, Digital Photography III, 65020O (20 February 2007), DOI: 10.1117/12.703485.

[3] Chiu C.W., Chao P.C.P., Wu D.Y., *Optimal design of magnetically actuated optical image stabilizer mechanism for cameras in mobile phones via genetic algorithm*, IEEE Transactions on Magnetics **43**(6), 2007, pp. 2582–2584, DOI: 10.1109/TMAG.2007.893320.

[4] Daniilidis K., Krauss C., Hansen M., Sommer G., *Real-time tracking of moving objects with an active camera*, Real-Time Imaging **4**(1), 1998, pp. 3–20, DOI: 10.1006/rtim.1996.0060.

[5] Oike H., Wu H., Hua C., Wada T., *Clear image capture-active cameras system for tracking a high -speed moving object*, [In] Proceedings of the Fourth International Conference on Informatics in Control, 2007, pp. 94–102.

[6] Okumura K., Oku H., Ishikawa M., *High-speed gaze controller for millisecond-order pan/tilt camera*, [In] Proceedings of IEEE International Conference on Robotics and Automation, 2011, pp. 6186–6191, DOI: 10.1109/ICRA.2011.5980080.

[7] Hayakawa T., Watanabe T., Ishikawa M., *Real-time high-speed motion blur compensation system based on back-and-forth motion control of galvanometer mirror*, Optics Express **23**(25), 2015, pp. 31648–31661, DOI: 10.1364/OE.23.031648.

[8] YITZHAKY Y., MILBERG R., YOHAEV S., KOPEIKA N.S., *Comparison of direct blind deconvolution methods for motion-blurred images*, Applied Optics **38**(20), 1999, pp. 4325–4332, DOI: 10.1364/AO.38.004325.

[9] ZHANG J., ZHANG Q., HE G., *Blind deconvolution of a noisy degraded image*, Applied Optics **48**(12), 2009, pp. 2350–2355, DOI: 10.1364/AO.48.002350.

[10] LEVIN A., SAND P., CHO T.S., DURAND F., FREEMAN W.T., *Motion-invariant photography*, ACM Transactions on Graphics **27**(3), 2008, pp. 1–9, DOI: 10.1145/1360612.1360670.

[11] ZHONG P., YU Q.Y., JIN G., *Motion estimation and motion compensation based on matching technology of feature point*, Journal of Optoelectronics Laser **15**(1), 2004, pp. 73–77.

[12] KUMAR S., AZARTASH H., BISWAS M., NGUYEN T., *Real-time affine global motion estimation using phase correlation and its application for digital image stabilization*, IEEE Transactions on Image Processing **20**(12), 2011, pp. 3406–3418, DOI: 10.1109/TIP.2011.2156420.

[13] PREVOST C.G., DESBIENS A., GAGNON E., *Extended Kalman filter for state estimation and trajectory prediction of a moving object detected by an unmanned aerial vehicle*, 2007 American Control Conference, IEEE, 2007, DOI: 10.1109/ACC.2007.4282823.

[14] FU H.X., LIU S., SUN F., *Ship motion prediction based on AGA-LSSVM*, 2010 IEEE International Conference on Mechatronics and Automation, 2010, DOI: 10.1109/ICMA.2010.5589093.

[15] ZHAO D., GAO Y., ZHANG Z., ZHANG Y., LUO T., *Prediction of vehicle motion based on Markov model*, [In] 2017 International Conference on Computer Systems, Electronics and Control (ICCSEC), 2017, pp. 205–209, DOI: 10.1109/ICCSEC.2017.8446749.

[16] GUO J.Q., HE H.W., SUN C., *ARIMA-based road gradient and vehicle velocity prediction for hybrid electric vehicle energy management*, IEEE Transactions on Vehicular Technology **68**(6), 2019, pp. 5309–5320, DOI: 10.1109/TVT.2019.2912893.

[17] QIAO S.J., HAN N., ZHU X.W., *et al.*, *A dynamic trajectory prediction algorithm based on Kalman filter*, Acta Electronica Sinica **46**(2), 2018, pp. 418–423.

[18] SIVANAGARAJA T., VELUVOLU K.C., *Respiratory motion prediction using moving window based online training approach for LS-SVM*, 2015 2nd International Conference on Signal Processing and Integrated Networks (SPIN), 2015, DOI: 10.1109/SPIN.2015.7095297.

[19] DHANYA, J., RAGHUKANTH S.T.G., *Ground motion prediction model using artificial neural network*, Pure and Applied Geophysics **175**(3), 2018, pp. 1035–1064, DOI: 10.1007/s00024-017-1751-3.

[20] CHENG X., CHEN S., DIAO C., LIU M., LI G., ZHANG H., *Simplifying neural network based model for ship motion prediction: a comparative study of sensitivity analysis*, International Conference on Offshore Mechanics and Arctic Engineering, American Society of Mechanical Engineers, 2017, DOI: 10.1115/OMAE2017-61474.

[21] FLORENT A., DE LA FORTELLE A., *An LSTM network for highway trajectory prediction*, 2017 IEEE 20th International Conference on Intelligent Transportation Systems (ITSC), 2017, DOI: 10.1109/ITSC.2017.8317913.

[22] ZHANG P., OUYANG W., ZHANG P., XUE J., ZHENG N., *SR-LSTM: state refinement for LSTM towards pedestrian trajectory prediction*, [In] Proceedings of the IEEE/CVF Conference on Computer Vision and Pattern Recognition 2019, pp. 12085–12094, DOI: 10.1109/CVPR.2019.01236.

Received April 13, 2021
in revised form June 7, 2021